Cell Communication and Signaling

RESEARCH

Open Access

Integrating transcriptomics, glycomics and glycoproteomics to characterize hepatitis B virus-associated hepatocellular carcinoma

Zhuo Li[1,2†], Na Zhang[1†], Zewen Dong[2], Xin Wang[1], Jian Zhou[1], Juan Gao[1], Yunyun Yang[2], Jing Li[2], Feng Guan[2], Yue Zhou[2*] and Zengqi Tan[3*]

Abstract

Background Hepatocellular carcinoma (HCC) ranks as the third most common cause of cancer related death globally, representing a substantial challenge to global healthcare systems. In China, the primary risk factor for HCC is the hepatitis B virus (HBV). Aberrant serum glycoconjugate levels have long been linked to the progression of HBV-associated HCC (HBV-HCC). Nevertheless, few study systematically explored the dysregulation of glycoconjugates in the progression of HBV-associated HCC and their potency as the diagnostic and prognostic biomarker.

Methods An integrated strategy that combined transcriptomics, glycomics, and glycoproteomics was employed to comprehensively investigate the dynamic alterations in glyco-genes, N-glycans, and glycoproteins in the progression of HBV- HCC.

Results Bioinformatic analysis of Gene Expression Omnibus (GEO) datasets uncovered dysregulation of fucosyltransferases (FUTs) in liver tissues from HCC patients compared to adjacent tissues. Glycomic analysis indicated an elevated level of fucosylated N-glycans, especially a progressive increase in fucosylation levels on IgA1 and IgG2 determined by glycoproteomic analysis.

Conclusions The findings indicate that the abnormal fucosylation plays a pivotal role in the progression of HBV-HCC. Systematic and integrative multi-omic analysis is anticipated to facilitate the discovery of aberrant glycoconjugates in tumor progression.

Keywords HBV-associated HCC, Transcriptomics, Glycomics, Glycoproteomics, Fucosylation

†Zhuo Li and Na Zhang contributed equally to this work.

*Correspondence:
Yue Zhou
yue.zhou@nwu.edu.cn
Zengqi Tan
zengqtan@nwu.edu.cn
[1] Department of Laboratory Medicine, The First Affiliated Hospital of Xi'an Medical University, Xi'an, Shaanxi 710077, P.R. China
[2] Key Laboratory of Resource Biology and Biotechnology in Western China, Ministry of Education, Provincial Key Laboratory of Biotechnology, College of Life Sciences, Northwest University, Xi'an, Shaanxi 710069, P.R. China
[3] Institute of Hematology, Provincial Key Laboratory of Biotechnology, School of Medicine, Northwest University, Xi'an, Shaanxi 710069, P.R. China

Introduction

Hepatocellular carcinoma (HCC) is a primary liver malignancy and ranks as the third leading cause of cancer-related death worldwide [1]. Hepatitis B and C viral infections are the two major etiologies of HCC [2, 3], with chronic HBV being predominating in China due to the high prevalence of HBV infection [4, 5]. The relative risk of HCC in HBV-positive patients compared to HBV-negative controls is much higher [6]. Most HBV-HCC patients experience a trilogy of hepatitis-cirrhosis-HCC [7, 8]. Alpha-fetoprotein (AFP) is the most commonly used serum biomarker for HCC since it was discovered in 1964 [9]. However, approximately 30% of patients with early-stage HCC are AFP negative [10], and elevated AFP levels are also detected in patients with cirrhosis or chronic HCV exacerbations [11]. Indeed, most cancer markers used in clinics are glycoproteins [12], and their glycan moieties may be structurally different in cancer [13]. Therefore, a global analysis of the precise variation of glycoconjugates in HBV- HCC is urgently needed.

Glycosylation is one of the most abundant and diverse protein post-translational modifications in eukaryotes, with profound effects on protein function, stability, subcellular localization and other traits [14]. N-glycosylation, the main form of protein glycosylation, was dysregulated in common diseases such as cancer [15–17], inflammation [18], Alzheimer's disease [19, 20] and diabetes [21–23]. Connor A West et al. reported that the levels of tetra-antennary and fucosylation was elevated in HCC tissues compared to either cirrhotic tissue or adjacent untransformed tissue [24]. N-glycans with β1,6-N-acetylglucosamine (β1,6-GlcNAc) branching and sialylated GlcNAc structures were increased in HCC cell line, Huh7 [25].

As one of the terminal modifications, fucosylation is the process of transferring fucose from GDP-fucose to their substrates by fucosyltransferases in all mammalian cells [26]. Recent studies revealed that levels of core and outer-armer fucosylation were increased in the serum of patients with HCC [27]. The cancer-promoting capacity of cancer-associated fibroblasts was facilitated by modifying EGFR core fucosylation in non-small cell lung cancer [28]. Some highly abundant serum proteins such as transferrin (TF) and alpha-1-anti-trypsin (A1AT) were found to be decorated with increased levels of fucosylation in HCC [29]. These results demonstrate that glycosylation shows the potential as an indicator of liver disease progression to HCC. However, these studies commonly focus on cancer and adjacent tissues, rather than the process of liver disease from healthy control to HCC. In addition, each omics approach, such as transcriptomics, glycomics and glycoproteomics, cannot capture the entire biological complexity of most human diseases. Therefore, an integration of multiple omics approaches can provide a more comprehensive information on biological significance and diagnostic potential of glycans in the process of HCC.

In this study, multi-omics including transcriptomics, glycomics, and glycoproteomics were integrated to profile the aberrant levels of glycan-related gene, glycan pattern, site-specific glycoproteins in HBV-HCC process.

Materials and methods

Patients and samples

Three pairs of HBV-HCC and adjacent tissues, and serum samples from 27 chronic hepatitis B (CHB), 22 HBV-related liver cirrhosis (LC), 31 HBV- HCC patients and 20 healthy controls (HC) were collected from The First Affiliated Hospital of Xi'an Medical University. Informed consent was conducted in accordance with Declaration of Helsinki and experiments were approved by The First Affiliated Hospital of Xi'an Medical University Ethics Committee. Characteristic of samples are listed in Table S1&2.

GEO data analysis

The gene expression profile data GSE135631 and GSE94660 was downloaded from GEO of the National Center for Biotechnology Information (NCBI). Gene expression data deposited as the Series Matrix data was used for analysis of the fold change of gene expression and *p* value.

Quantitative reverse transcription PCR (RT-qPCR)

RNA from the indicated tissues was extracted using Trizol (ABclonal; Wuhan, Hubei, China) and reversed transcribed using the cDNA Reverse Transcription Kit (ABclonal). RT-qPCR was performed using SYBR Green Master Mix using Real-Time PCR system (TIANLONG; Xi'an, Shaanxi, China). Primer sequences were provided in Table S3.

Analysis of N-glycans

Glycomic analysis was performed as previously described [30]. A volume of 10 µL serum was added onto a size-exclusion spin ultrafiltration unit (Millipore; Billerica, MA, USA). Proteins were denatured with 8 M urea/50 mM NH_4HCO_3, reduced with dithiothreitol (DTT), alkylated with iodoacetamide (IAM), and digested with PNGase F overnight at 37 °C. Released N-glycans were collected by centrifugation, lyophilized, and desalted using HyperSep Hypercarb solid phase extraction (SPE) cartridge (ThermoFisher Scientific; Waltham, Massachusetts, US).

Lyophilized N-glycans were dissolved and spotted onto an MTP AnchorChip sample target with 20 mg/

mL 2,5-dihydroxybenzoic acid (DHB) as the matrix. Measurements were taken in positive-ion mode. Each full-mass scan was performed with following conditions: acceleration voltage, 24.59 kV; reflector voltage, 26.6 kV; pulsed ion extraction, 100 ns; mass range, 1000–3500 m/*z*. For the data analysis, the peaks were smoothed and baseline subtraction performed three times. Relative intensity was analyzed and generated using FlexAnalysis software (Bruker Daltonics; Bremen, Germany) based on MALDI-TOF/TOF–MS intensity. *m/z* data were obtained and annotated using GlycoWorkbench software program [31], cross-referenced with previous studies [32–34], together with knowledge of mammalian glycan biosynthetic pathway products. For the isomeric structures that are not easily deciphered by MALDI-TOF–MS, uncertainties in sequences, especially fuzzily defined capping unit locations, have been indicated outside the bracket in the proposed N-glycan structure.

Proteomics and glycoproteomics

Protein extraction and digestion was performed as previously described [30]. In brief, the serum protein was denatured in 8 M urea/ 50 mM NH_4HCO_3, then reduced with DTT, alkylated with IAM, digested with lysyl endopeptidase (Promega; Madison, WI, USA) for 4 h at 37 °C, and then incubated with trypsin (Promega) overnight at 37 °C with shaking. The digested peptides were acidified with 10% trifluoroacetic acid to pH < 3, collected by centrifugation and purified using Oasis HLB cartridges (Waters; Milford, MA, USA). Desalted peptides were subjected to LC–MS/MS analysis for proteomics. N-glycopeptides were enriched by MAX column (Waters) using desalted peptides, and subjected to LC–MS/MS analysis for glycoproteomics as described previously [35].

Enzyme-Linked Immunosorbent Assay (ELISA)

To determine the Igs levels in serum, direct ELISA was applied. ELISA plates were coated with serum sample for 2 h at 37 °C, blocked with 3% BSA in PBS for 2 h at room temperature (RT), rinsed with PBST, incubated with antibody against IgA1 or IgG2 (Abcam; Cambridge, MA, USA) for 2 h at 37 °C, rinsed with PBST, incubated with secondary antibody for 30 min at RT, rinsed with PBST, and visualized with TMB substrate kit (Beyotime Institute of Biotechonology; Haimen, China). The absorbance values were determined at 450 nm with a plate reader.

To determine the glycosylation on Igs, sandwich ELISA was performed. ELISA plates were coated with antibodies against IgA1 or IgG2 overnight at 4 °C, rinsed with PBST, blocked with 5% BSA, incubated with serum samples for 2 h at 37 °C, rinsed with PBST, incubated with biotinylated lectins (Vector Labs) overnight at 4 °C, incubated with VECTASTAIN ABC reagent for 30 min at RT, and visualized with TMB substrate solution. The absorbance values were determined at 450 nm with a plate reader.

Data analysis

All experiments were reproduced at least three times. All values were presented as mean ± standard deviation (SD). Two-tailed Student's t-test was used for comparison of data sets between two groups and differences with $p < 0.05$ were considered statistically significant. Statistical analysis was performed using GraphPad Prism 9.3.1 software program.

Results

Glycan-related genes expression of HBV-HCC and adjacent tissues

A better understanding of glyco-gene expression changes may facilitate the exploration of association between glycosylation and HBV-HCC. The differences in glyco-gene expression and glycosylation in HBV-HCC were investigated using an integrated strategy with a combination of transcriptomics, glycomics and glycoproteomics (Fig. 1A). First, GSE135631 and GSE94660 gene expression profiles, including 15 and 21 pairs of HBV-HCC and adjacent tissues respectively, were retrieved from the GEO database. A total of 7502 and 7839 genes were differentially expressed in GSE135631 and GSE94660, as shown in Fig. 1B, in which top 100 differentially expressed glyco-genes (DEGGs) were highlighted (Fig. 1B, Table S4). Partial Least Squares Discrimination Analysis (PLS-DA) of these DEGGs exhibited a clear separation of HBV-HCC from adjacent tissues (Fig. 1C). The expression patterns of all DEGGs across HBV-HCC and adjacent tissues from the combined two GSE study

(See figure on next page.)

Fig. 1 Differentially expressed glycan-related genes in HBV-related HCC of GSE135631 and GSE94660. **A** Workflow of the present study. **B** Volcano plot of expression patterns of identified genes in GSE135631 and GSE94660. Red dots: up-regulated genes. Green dots: down-regulated genes. Highlighted dots: DEGGs. The q value (log10) is plotted against the log10 (FC: HBV-HCC tissues vs. adjacent tissues) using the cut-offs of fold change > 1.5 or < 0.67 and *p* value < 0.05. **C** PLS-DA plot of DEGGs in GSE135631 and GSE94660. **D** Heatmap showing the expression pattern of DEGGs in HBV-HCC and adjacent tissues of GSE135631 and GSE94660. **E** Functional enrichment analysis of DEGGs. **F** The PPI network of DEGGs performed by the STRING database and cytoscape tools. The red colour intensity was proportional to the degree of connectivity. **G** The mRNA expression of 13 FUTs, PIGV, PIGT, PIGM and B4GALT3 genes in 3 pairs of HBV-HCC and adjacent tissues determined by RT-qPCR

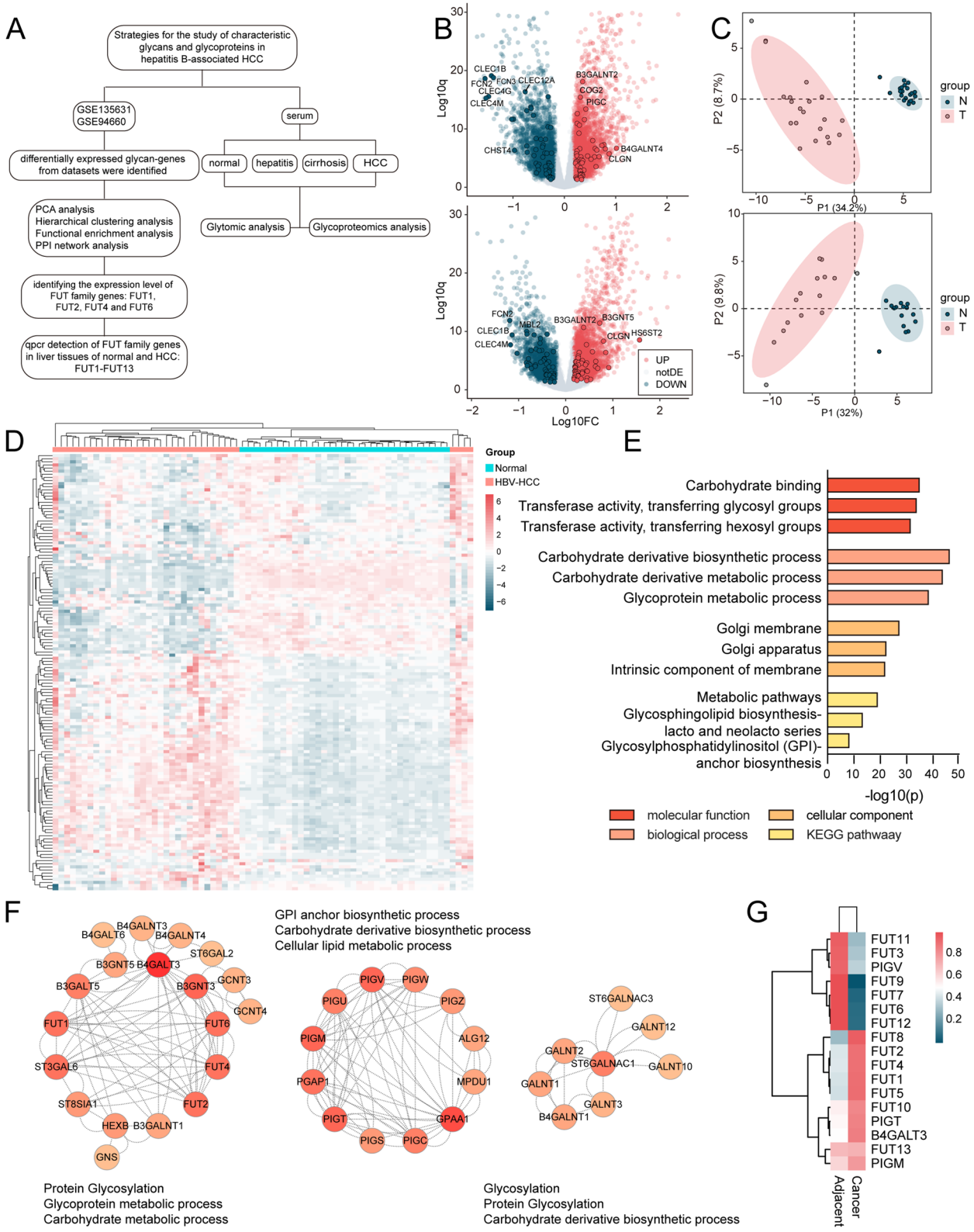

Fig. 1 (See legend on previous page.)

were shown as a heatmap (Fig. 1D). Next, functional enrichment analysis revealed that the main molecular function categories were carbohydrate binding, transferring glycosyl and hexosyl group activity (Fig. 1E). Protein–protein interaction (PPI) network of these DEGGs was constructed in an attempt to explicit the molecular mechanisms in the progression of HBV-HCC. Clustering analysis revealed ten major modules, in which protein glycosylation, GPI anchor biosynthetic process and glycosylation processes were mostly enriched (Fig. 1F; S1). Hub genes with a high degree of connectivity in the PPI network are significantly enriched in the process of fucosylation (FUT4, FUT6, FUT2 and FUT1), GPI anchor biosynthesis (PIGM, PIGV, PIGT and GPAA1), galactosylation (B4GALT3) and galNAcylation (B3GNT3).

Furthermore, FUTs family expression at mRNA levels were determined by RT-qPCR in HBV-HCC and adjacent tissues (Fig. 1G), revealed an elevated level of FUT1, FUT2, FUT4, FUT5, FUT8, FUT10, PIGT, PIGM and B4GALT3, as well as a reduced level of FUT3, FUT6, FUT7, FUT9, FUT11, FUT12 and PIGV in HBV-HCC tissues. Although HCC and adjacent tissue samples in transcriptomic analysis can not represent the whole HCC progression, these data provide clues in understanding dysregulated glycosylation especially fucosylation in HBV-HCC.

N-glycan profiles of normal, hepatitis, cirrhosis and HCC serum samples

In our studies, N-glycans in HC, CHB, LC and HBV-HCC serum samples (Tab. S1) were profiled by MALDI-TOF/TOF–MS to reveal abnormal N-glycosylation. Representative MS spectra of N-glycans with signal-to-noise ratios > 5 were displayed and annotated (Fig. 2; Table S5). A total of 36 distinct *m/z* N-glycan structures were identified, with 31, 32, 25 and 25 N-glycans present in HC, CHB, LC and HBV-HCC samples, respectively. There were 21 N-glycans found in all groups but with different intensities.

The expression pattern of identified N-glycans in HC, CHB, LC and HBV-HCC were exhibited in Fig. 3A. Hierarchical clustering revealed that LC/HBV-HCC were clearly separated from HC and CHB, however, LC/HBV-HCC could not be separated from each other. Furthermore, quantitative comparison analysis revealed that 25, 24, and 22 N-glycan structures were differentially expressed in CHB, LC and HBV-HCC versus HC. Of these N-glycans, 11 N-glycans were concertedly

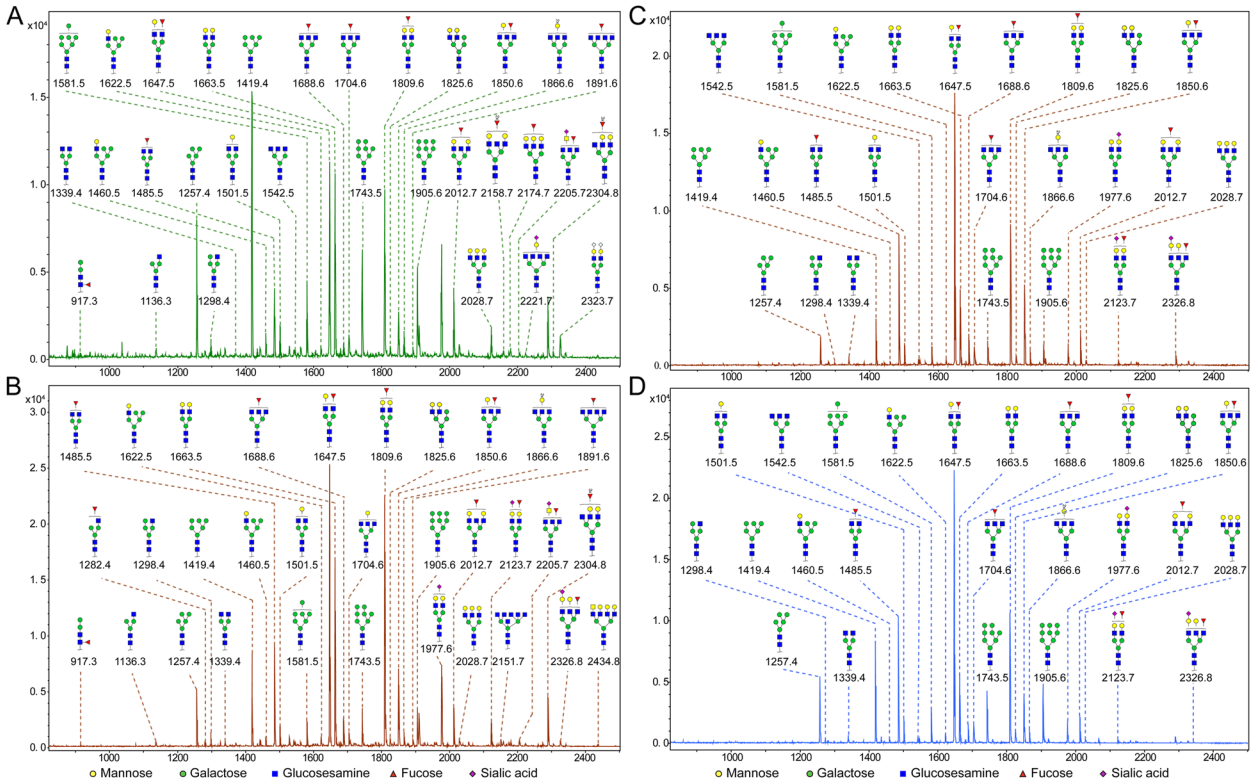

Fig. 2 MALDI-TOF/TOF–MS spectra of N-glycans in HC, CHB, LC and HBV-HCC serum samples. Peaks of MALDI-TOF/TOF–MS spectra (signal-to-noise ratio > 5) were selected for relative intensity analysis in HC (**A**), CHB (**B**), LC (**C**) and HBV-HCC (**D**) samples. Detailed structures were annotated with GlycoWorkbench software. Proposed structures are indicated by *m/z* value

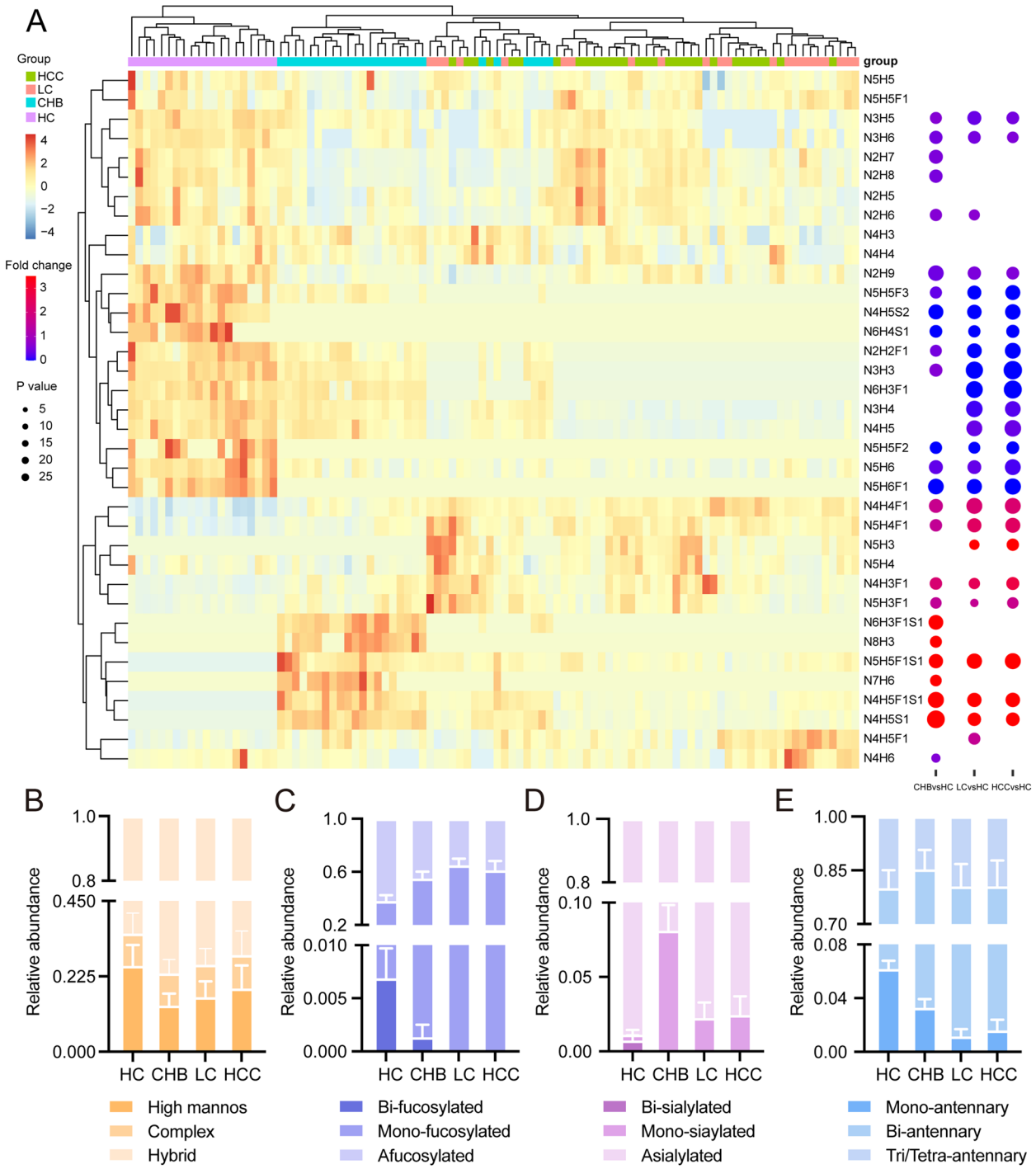

Fig. 3 N-glycan levels in HC, CHB, LC and HBV-HCC serum samples. **A** Expression pattern and dysregulation of N-glycans identified in HC, CHB, LC and HBV-HCC. **B** Relative abundances of high mannose, complex and hybrid N-glycans. The relative abundance is calculated by adding the relative abundances of a given type of N-glycan. **C** Relative abundances of bi-, mono- and afucosylated N-glycans. **D** Relative abundances of bi-, mono- and asialylated N-glycans. **E** Relative abundances of N-glycans with mono-, bi- and tri/tetra-antennary structures

down-regulated, and 7 N-glycans were concertedly up-regulated in the progression of HBV-HCC. Notably, All up-regulated N-glycans were fucosylated (Fig. 3A; Table S5).

N-glycans were classified into three types, including high mannose, complex and hybrid. Relative abundance of hybrid and complex N-glycans were increased in CHB, LC and HBV-HCC versus HC, while which of high mannose N-glycans were decreased (Fig. 3B). Consistent with elevated FUTs expression at mRNA levels, relative abundance of total fucosylation were up-regulated, of which mono-fucosylation levels were increased, while bi-fucosylation levels were decreased (Fig. 3C). Other terminal modification sialylation levels were increased, followed by a decrease in the progression of HBV-HCC (Fig. 3D). Significantly higher levels of bi-antennary structures were found in CHB, LC and HBV-HCC versus HC, while mono-antennary structures was progressively reduced (Fig. 3E). In combination of transcriptomic and glycomic analysis revealed that fucosylation levels were up-regulated in the progression of HBV-HCC.

Site-specific glycoproteomic profiling in HBV-HCC serum samples

To decode the biological function of specific N-glycosylation especially fucosylation in the progression of HBV-HCC, intact glycoproteomic analysis of HC, CHB, LC and HBV-HCC serum samples (Table S2) were performed. A total of 1114 glycopeptides were identified (Fig. 4A; Table S6), of which, 1019, 1011, 999 and 982 glycopeptides, including 864 in common were found in HC, CHB, LC and HBV-HCC serum samples, respectively. The identified glycopeptides represented 129 glycosites were modified with 102 glycan structures. These N-glycans contained 8 high mannose, 13 hybrid, 77 complex and 4 paucimannose subtypes (Fig. 4B).

Quantitative comparison analysis revealed that 116, 197 and 192 glycopeptides were differentially expressed in HC compared to CHB, LC and HCC, respectively, using the cutoff of fold change > 1.5 or < 0.67 and p

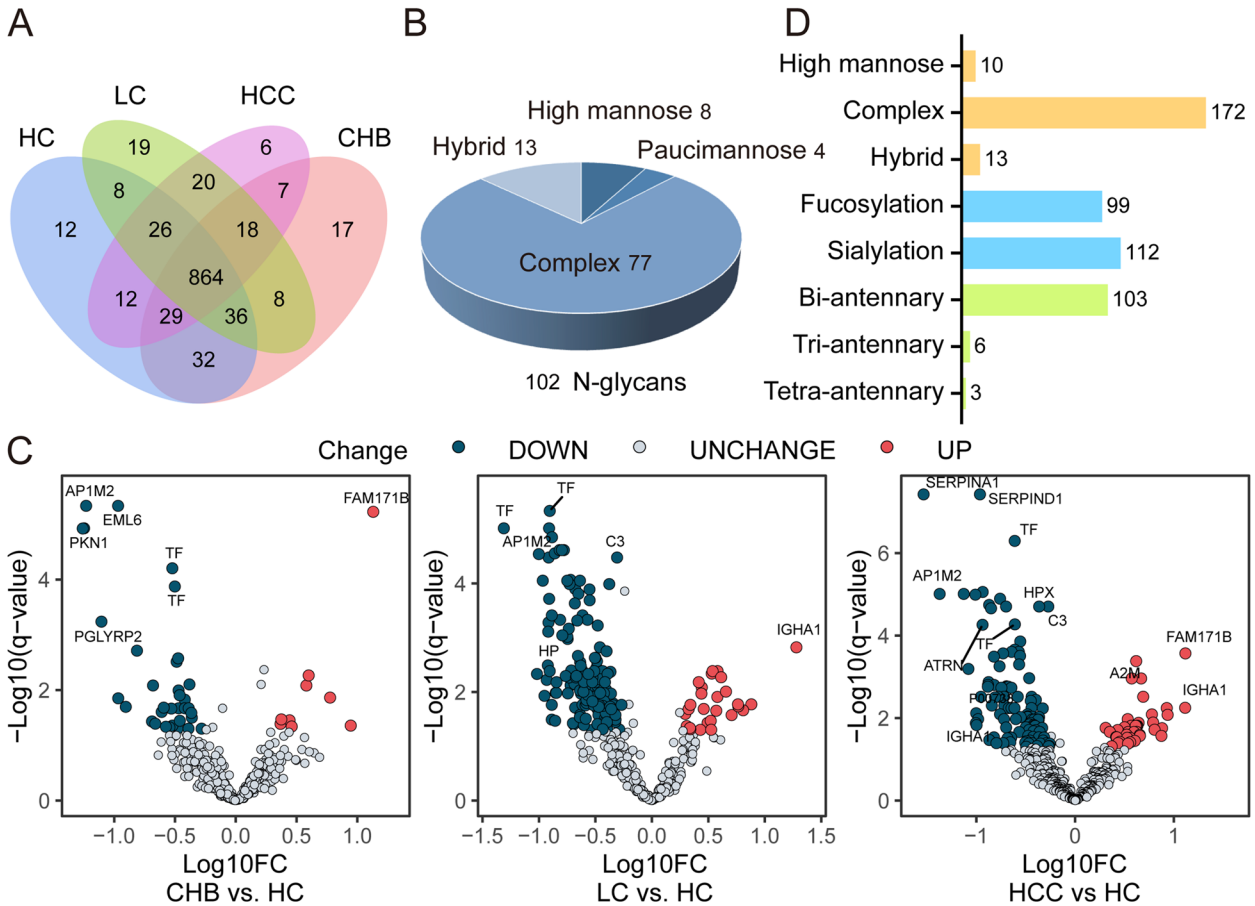

Fig. 4 Quantitative glycoprotemic analysis of HC, CHB, LC and HBV-HCC serum samples. **A** Venn diagram of intact glycopeptides identified from HC, CHB, LC and HBV-HCC samples. **B** Distribution of glycan subtypes from intact glycopeptides identified from HC, CHB, LC and HBV-HCC samples. **C** Volcano plots of expression patterns of identified glycopeptides. Red dots: up-regulated glycopeptides. Green dots: down-regulated glycopeptides. The value q (-log10) is plotted against the log10 (FC: disease group vs. normal group). **D** Classification of differentially expressed intact glycopeptides based on their attached glycan structures. The numbers indicate the unique glycopeptides modified by the corresponding glycans

value < 0.05 (Fig. 4C). These 288 differentially expressed glycopeptides (DEGPeps) from 73 glycoproteins were mainly decorated with complex type N-glycans, of which sialylated N-glycans accounted for the largest proportion, followed by fucosylated N-glycans and bi-antennary structures (Fig. 4D).

To understand the association between glycoprotein trajectories and the progression of HBV-HCC, hierarchical clustering for all DEGPeps was performed, with which four cluster (I-IV) were generated (Fig. 5A&B; Table S7). Glycopeptides in "cluster I" were continually increased in the progression of HBV-HCC, encompassing 27 proteins. These DEGPeps were significantly

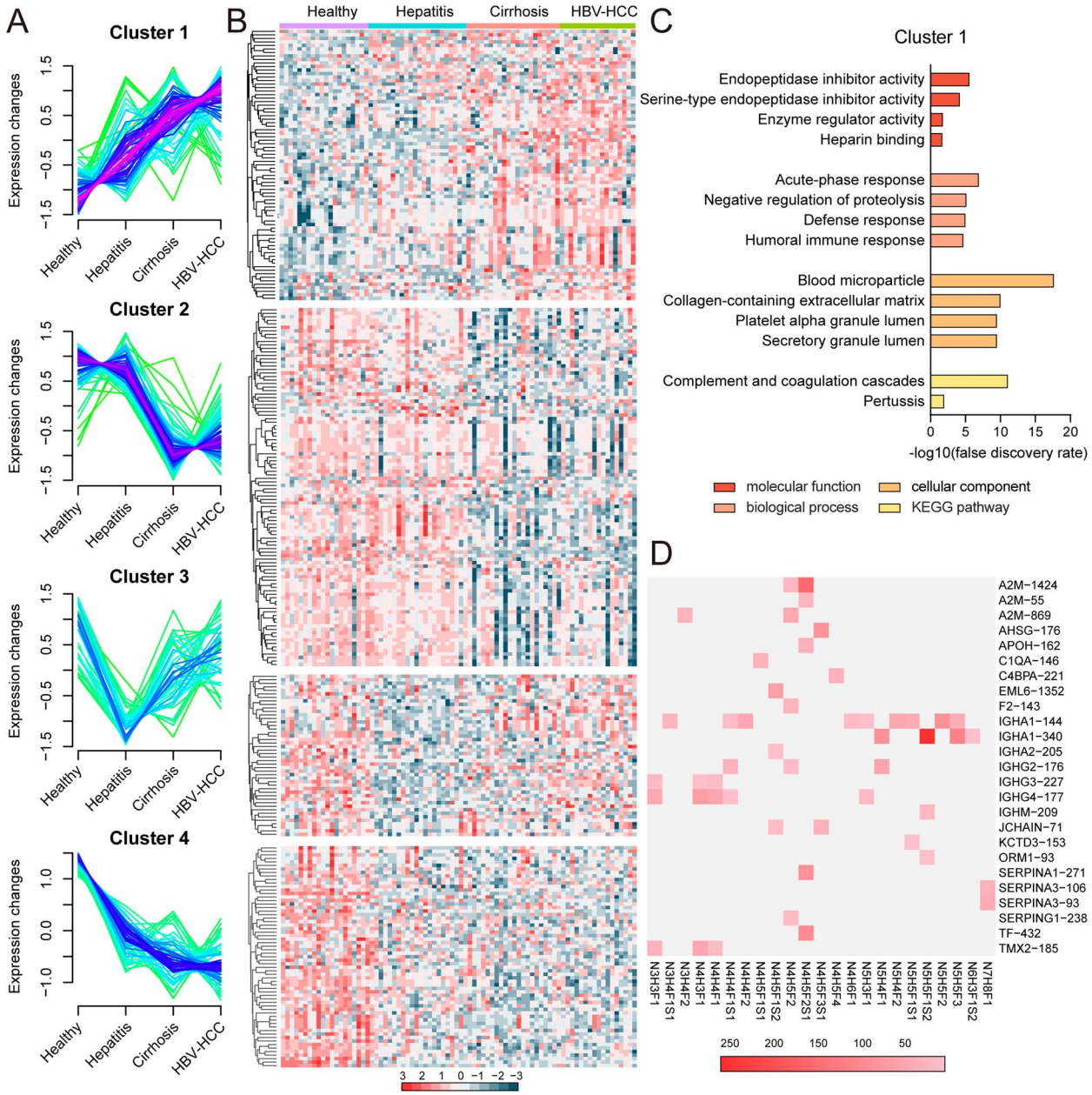

Fig. 5 Hierarchical clustering analysis of differentially expressed glycopeptides identified in HC, CHB, LC and HBV-HCC. **A** Mfuzz clustering of differentially expressed glycopeptides. **B** Expression pattern of glycopeptides from cluster I, II, III and IV. **C** Functional enrichment analysis of differentially expressed glycopeptides from cluster I. **D** Heatmap of fucosylated N-glycans on intact glycopeptides from cluster I. PSMs of the intact glycopeptides, comprising of different glycans (bottom) and their glycosite locations in different glycoproteins (right) are exhibited in the heat map

enriched in endopeptidase inhibitor activity, acute-phase response, blood microparticle and complement and coagulation cascades by functional enrichment analysis (Fig. 5C). Glycopeptides in "cluster II" were significantly decreased, followed by an increase (39 proteins), and mainly involved in the peptidase regulator activity, complement activation, blood microparticle and complement and coagulation cascades. Glycopeptides in "cluster III" were slightly decreased, followed by an increase (25 proteins), and enriched in regulation of humoral immune response, blood microparticle and complement and coagulation cascades. Glycopeptides in "cluster IV" (31 proteins) were decreased and primarily connected with peptidase regulator activity, acute-phase response, blood microparticle, complement and coagulation cascades. (Fig. S2).

Taking into account the escalating malignancy of HBV-HCC progression, 49 glycopeptides with fucosylation attached in "cluster I" were screened out, which were consisted of 23 fucosylated N-glycans and 25 peptides from 21 protiens (Fig. 5D). These fucosylated N-glycans contained three to seven HexNAc, three to eight hexose, up to four fucose, and two sialic acid. Among 21 identified glycoproteins, 16 contained 1 glycosite, 3 contained 2 glycosites, and 1 contained 3 glycosites. Notably, among these glycopeptides, IgA1-340-N5H5F1S2 was identified with highest PSM score.

Site-specific fucosylation on IgA1 and IgG2

We further mapped N-glycan structures on each glycosite of DEGPeps from IgA1 and IgG2 based on our glycoproteomics data. A total of 30 and 5 unique intact glycopeptides were identified from IgA1 and IgG2, which were comprised 3 glycosites (^{144}N$^{\#}$LT and ^{340}N$^{\#}$VS for IgA1, ^{176}N$^{\#}$ST for IgG2) and 31 glycans (Fig. 6A). Among these glycopeptides, fucosylation was accounted for 46% of all glycans on glycopeptides, and the majority of fucosylated intact glycopeptides were up-regulated in the progression of HBV-HCC.

Among these DEGPeps, 7 and 3 site-specific fucosylated glycopeptides from IgA1 and IgG2, showed a directionally concerted up-regulation in the HC-CHB-LC-HCC progression (Fig. 7A). To evaluate the diagnostic value of the aberrant fucosylated Igs in clinical practice, lectin-based ELISA assay with *Concanavalin A* (ConA), *Lens Culinaris* Agglutinin (LCA) and *Aleuria Aurantia* Lectin (AAL) was performed, which respectively recognize high mannose type N-glycans, α1,6-fucose, and α1,2/α1,3/α1,4/α1,6-fucose. The results revealed that total levels of IgG2 and IgA1 were not significantly changed, and different glycoform on Igs exhibited different expression patterns in the progression of HBV-HCC (Fig. 7B). AAL-reactive IgA1 and IgG2 were significantly elevated in HBV-HCC compared to HC, CHB and LC. LCA-reactive IgA1 was increased in HBV-HCC when

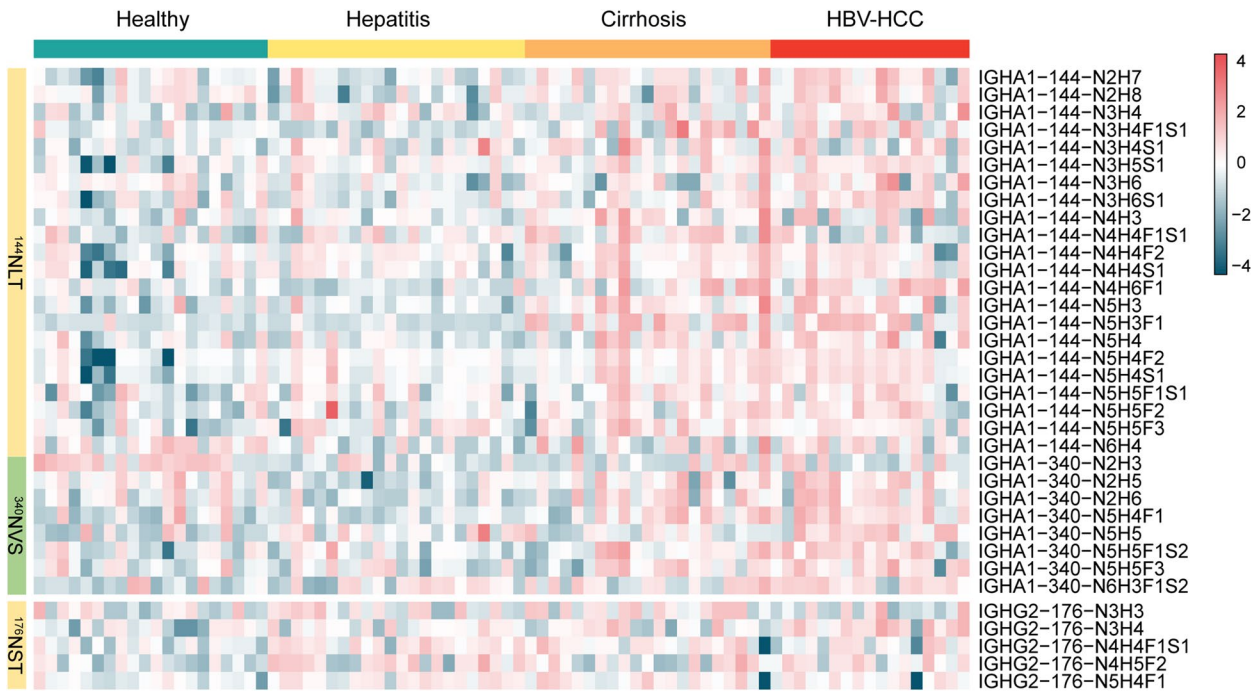

Fig. 6 Site-specific glycan profiling of IGHA1 and IGHG2 identified in HC, CHB, LC and HBV-HCC. Heatmap showing all the identified glycans at the glycosite Asn-144, Asn-340 of IGHA1, and Asn-176 of IGHG2

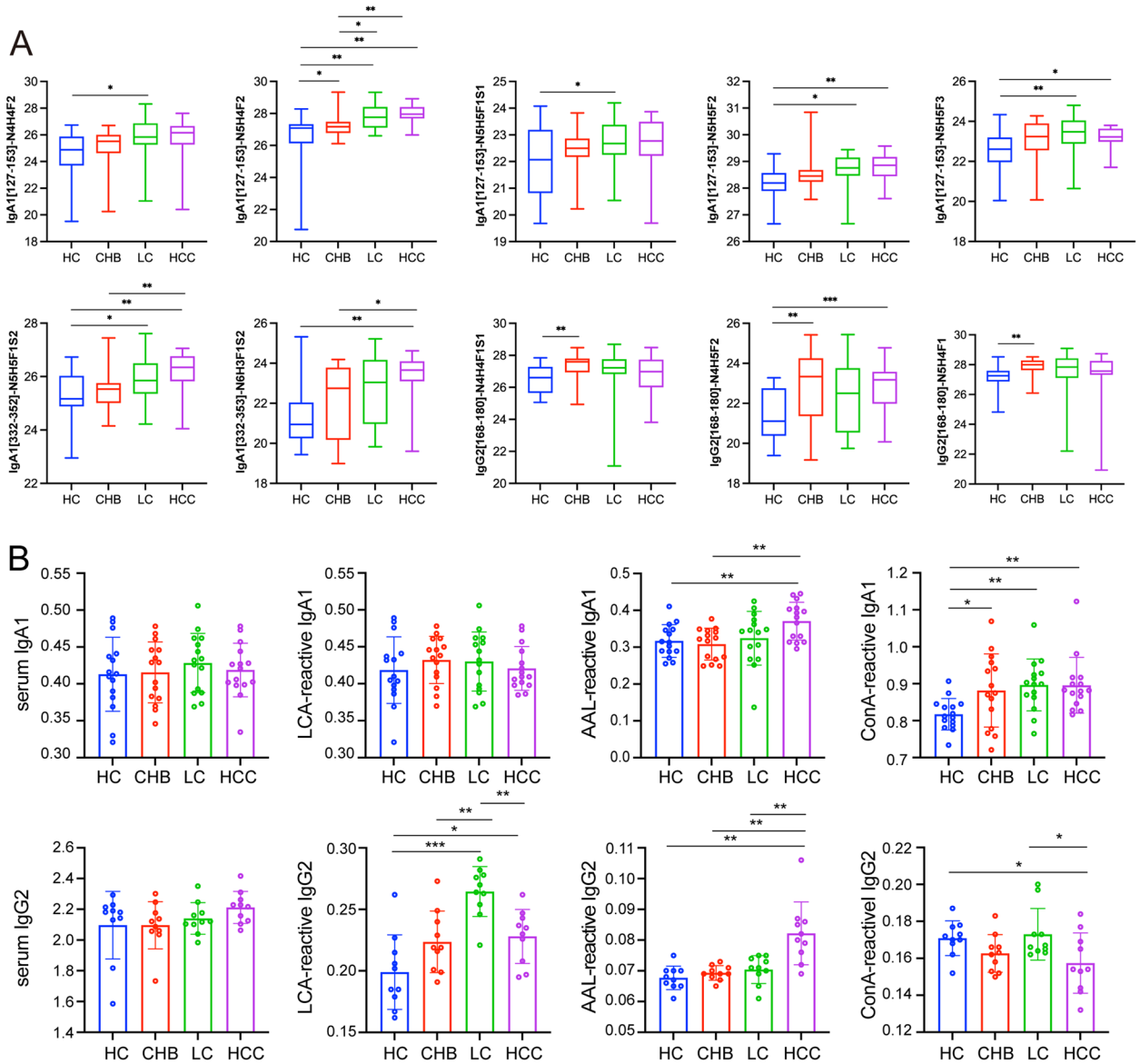

Fig. 7 Differentially expressed intact glycopeptides of IGHA1 and IGHG2. **A** Box plots of 10 site-specific fucosylated glycopeptides from IgA1 and IgG2 showed a directionally concerted up-regulation in the HC-CHB-LC-HCC progression. **B** Relative expression of IgA1/ IgG2 and ConA-/ LCA-/ AAL-reactive IgA1/ IgG2 in the HC, CHB, LC and HBV-HCC serum determined by ELISA

compared to HC and decreased compared to CHB and LC, and LCA-reactive IgG2 was gradually increased and followed by a decrease in the progression of HBV-HCC. ConA-reactive IgA1 were increased in CHB, LC and HBV-HCC compared to HC, and ConA-reactive IgG2 showed lowest levels in HBV-HCC group. The different performance of these different glycoform on Igs indicated that glycosylation on Igs were specifically altered in the progression of HBV-HCC.

In summary, combined results of glycoproteomic and ELISA analysis revealed that IgA1 and IgG2 are highly fucosylated and AAL-reactive fucosylated IgA1 and IgG2 were up-regulated in HBV-HCC, implying their potential diagnostic value.

Proteomic analysis of HBV-HCC serum samples

To comprehend the potential of the glycoproteins analysis and conclusions, proteomics of these samples have been performed, revealing 78, 163, and 186 differentially expressed proteins in HC compared to CHB, LC and HCC, respectively (Fig. 8A, Table S8). Among these differentially expressed proteins, 21 proteins, including AFP

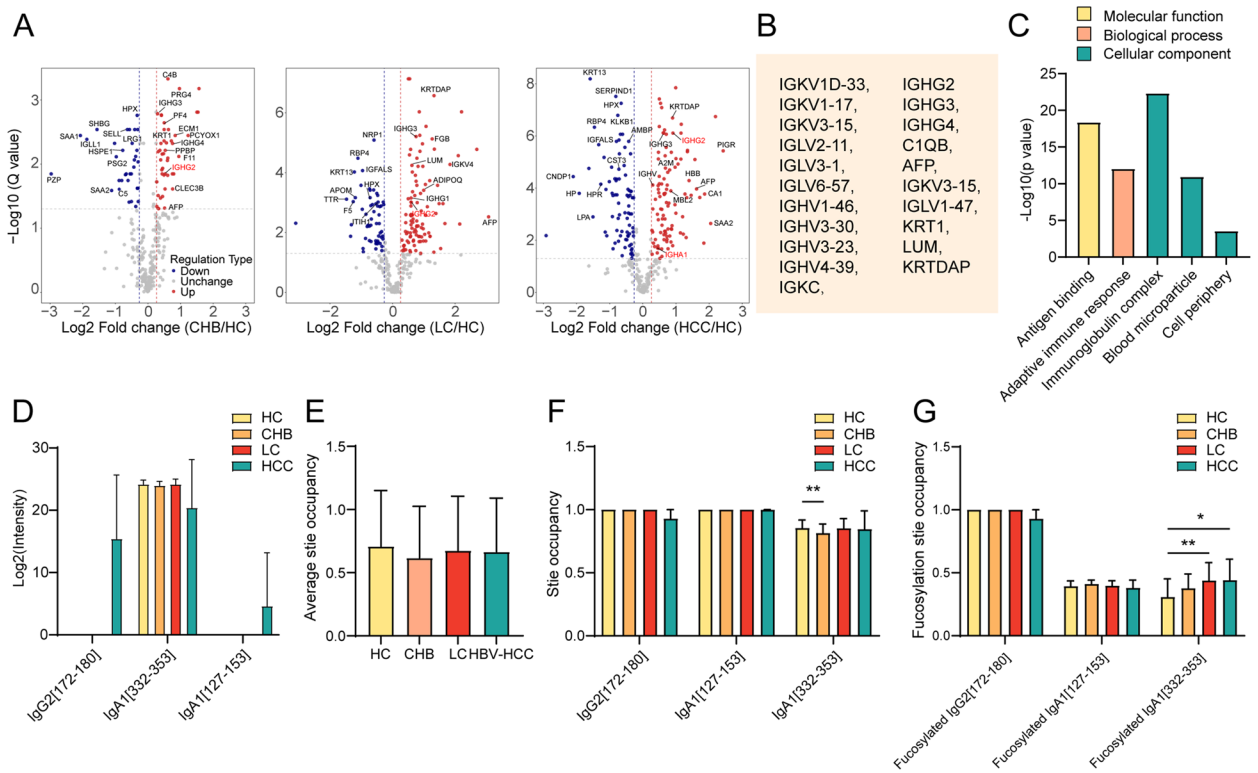

Fig. 8 Glycosylation site occupancy. **A** Volcano plots of expression patterns of identified proteins. Red dots: up-regulated proteins. Green dots: down-regulated proteins. The value q (-log10) is plotted against the log2 (FC: disease group vs. normal group). **B** Lists of concertedly up-regulated proteins in patients with liver disease (CHB, LC, or HBV-HCC) compared to HC. **C** GO enrichment analysis of the concertedly up-regulated proteins in HBV-HCC. **D** Levels of peptides from IgA1 and IgG2, including IgA1[127–153], IgA1[332–353] and IgG2[168–180] in HC, CHB, LC and HBV-HCC. **E** Average glycosylation site occupancy in HC, CHB, LC and HBV-HCC. Glycosylation site occupancy was calculated by dividing the abundance of a given type of glycoform by the total corresponding peptide (glycopeptide and non-glycopeptide) abundance. **F** Glycosylation site occupancy of IgA1[127–153], IgA1[332–353] and IgG2[168–180]. **G** Fucosylation site occupancy of IgA1[127–153], IgA1[332–353] and IgG2[168–180]

and diverse Igs, were up-regulated ($p < 0.05$) in patients with liver disease (CHB, LC, or HBV-HCC) compared to HC (Fig. 8B), that were mainly enriched in the cellular components of immunoglobulin complex, blood microparticle and cell periphery, the biological process of adaptive immune response, and molecular function of antigen binding (Fig. 8C). Notably, IgA1 did not show significant differences, while IgG2 was significantly up-regulated in patients with liver disease compared to HC (Fig. 8B). Peptides corresponding to the differentially expressed glycopeptides of Igs were investigated. The non-glycosylated peptides from IgA1 (amino acids 332–353; termed as IgA1[332–353]) did not show significant differences in the progression of HBV-HCC, while IgA1[127–153] and IgG2[172–180] were only detected in HBV-HCC (Fig. 8D), suggesting that fucosylated peptides from IgA1 and IgG2, especially IgA1[332–353], were specially up-regulated in the progression of HBV-HCC.

Furthermore, we correlated the abundance of glycopeptides with total corresponding peptides levels to determine the glycosylation site occupancy (Table S9). We found that the average site occupancy did not significantly changed (Fig. 8E). The glycosylation site occupancy of IgA1[127–153] and IgG2[172–180] exhibited no significant changes in the progression of HBV-HCC, and which of IgA1[332–353] was decreased in CHB compared to HC (Fig. 8F). Specifically, N-glycans on IgG2[172–180] were mainly fucosylated, and fucosylation site occupancy of IgA1[332–353] was elevated in LC and HCC compared to HC (Fig. 8G).

Collectively, When the IgA1 remains unchanged at protein levels, the fucosylation site occupancy of IgA1[332–353] increases, leading to a rise in IgA1[332–352]-N5H5F1S2 or -N6H3F1S2 and consequently resulting in elevated levels of AAL-reactive IgA1 in HBV-HCC. When fucosylation site occupancy of IgG2[168–180] remains unchanged, the IgG2 exhibited a upregulation at protein levels, contributing to a rise in IgG2[168–180]-N4H5F2 and consequently leading to a elevated level of LCA- and AAL-reactive IgG2 in HBV-HCC.

Discussion

An alteration in glycosylation have long been observed with the progression of HBV-HCC [36, 37]. Our study comprehensively characterizes the transcriptomics, glycomics and glycoproteomics landscapes of HC, CHB, LC and HBV-HCC, which allows us to interrogate underlying mechanisms in HBV-HCC progression. Our transcriptomic analysis revealed that several FUTs responsible for the N-glycan fucosylation were dysregulated in HBV-HCC (Fig. 1F). FUT1 catalyzes the addition of fucose to a terminal galactose in an α1,2-linkage, while FUT4, 6, 7, 9 catalyze the formation of α1,3-fucosylation on terminal GlcNAc, and FUT8 catalyze the core-α1,6-fucosylation on the innermost GlcNAc of core pentasaccharide. Consistently, our glycomic analysis revealed that most of concertedly up-regulated N-glycans in the progression of HBV-HCC were annotated to be fucosylated (Fig. 3C), in line with the up-regulation of FUT1, 4, 8. Recent studies also observed an elevated serum core-fucosylation by HPLC [38], and an elevated saliva fucosylation by saliva microarrays with *Lotus Tetragonolobus* Lectin [39] in the progression of human HBV-HCC. Moreover, a serum-associated fucosylated glycoprotein (< 10 kD) fingerprint was established to assist the diagnosis of HBV-HCC by using MALDI-TOF–MS, which could distinguish HBV-HCC from healthy subjects, patients with HBV and HBV-associated cirrhosis [40].

Furthermore, we found that most of concertedly up-regulated N-glycans were decorated with mono-fucosylated bi-/tri-antennary. Specifically, the up-regulation of the core-fucosylated monogalactose biantennary glycan (N4H4F1) is in agreement with the previously reported study [34]. In situ glycan imaging also revealed that fucosylation mostly on tetra-antennary and to a lesser extent on bi-antennary and tri-antennary glycans were elevated in HCC [24] in line with the elevated fucosylated tri-antennary N-glycans (N5H3F1, N5H4F1, N5H5F1) in our glycomic analysis. Xue-En Liu et al. found that a branch α1,3-fucosylated tri-antennary N-glycan (NA3Fb) was elevated in patients with HBV-HCC compared to who with HBV-fibrosis or cirrhosis or healthy subjects by using a DNA sequencer [41], furthermore, the log ratio of NA3Fb/NG1A2F was elevated in HBV-HCC, which was promising as N-glycan markers [42]. While, we found that levels of N5H6F1 N-glycan (the same component as NA3Fb) were reduced in HBV-HCC. This discrepancy might arise from inefficient distinction between N-glycan isoforms of MALDI-TOF–MS.

Advances in glycomics, genomics and proteomics platforms over the last decade have discovered numerous novel biomarkers and have improved the diagnosis of HBV-HCC. In recent years, the glycoproteome mapping provides innovative insights into the both peptides and glycosylation status in diseases and contributes to biomarker discovery. As the predominant constituent in immune molecule, Ig glycosylation especially fucosylation variations were found to be closely associated with the development of HBV-HCC using glycoproteomics [43]. Core-fucosylated serum IgG was significantly increased in HBV-HCC compared to HBV-related cirrhosis, HBV carriers and healthy subjects, and have general diagnostic performance than AFP in the training set and validation cohorts [44]. Similar research revealed that TPLTAN^{205}ITK (H5N5S1F1) and (H5N4S2F1) of IgA2 were significantly elevated in serum from patients with HBV infection and even higher in HBV cirrhosis in comparison with healthy donor [45]. Consistently, in the present study, 30 N-glycan structures on 2 glycosites of IgA1 and 5 N-glycans on 1 glycosite of IgG2 were identified. Specifically, differentially expressed IgA1 with fucosylated glycan structures (IgA1-144-N4H4F2/N5H4F2/N5H5F1S1/N5H5F2/N5H5F3 and IgA1-340-N5H5F1S2/N5H5F3/N6H3F1S2) and IgG2 with fucosylated glycan structures (IgG2-176-N4H3F1/N4H4F1/N5H3F1) were elevated in the progression of HBV-HCC determined by glycoproteomics.

Since each fucosylated glycoform can be recognized by a distinct lectin, a lectin-based ELISA was used to quantify the fucosylated Igs, which is more appropriate for the clinical practice. The present study revealed that the elevated AAL-reactive IgA1 and IgG2 in HBV-HCC might distinguish HBV-HCC from HC, CHB and LC. Similarly, the reduced LCA-reactive IgA1 in HBV-HCC might distinguish HBV-HCC from other groups, while the elevated LCA-reactive IgG2 in CHB, LC and HBV-HCC might distinguish liver diseases from HC, and even distinguish LC from other groups. These results indicated that LCA- and AAL-reactive Igs showed a diagnostic potential in distinguishing HBV-HCC from HC, CHB and LC.

By integrating omics and ELISA data, IgG2 levels were continuously elevated in patients with liver disease (CHB, LC, or HBV-HCC) compared to HC determined by proteomics (Fig. 8B), and which was slightly but not significantly increased in liver disease determined by ELISA (Fig. 7B). Notably, AAL- and LCA-reactive IgG2 were significantly elevated in HBV-HCC compared to HC (Fig. 7B), which might attribute to the changes in IgG2-176-HexNAc(4)Hex(5)Fuc(2) (Fig. 7A). Moreover, LCA-reactive IgG2 were up-regulated in CHB compared to HC (Fig. 7B), which might result from the variants of fucosylated glycopeptides including IgG-176-HexNAc(4)Hex(4)Fuc(1)NeuAc(1), HexNAc(4)Hex(5)Fuc(2), and HexNAc(5)Hex(4)Fuc(1) (Fig. 7B). These results reveal a specific expression pattern of fucosylated IgGs, distinct

from non-glycosylated IgGs, indicating their potential diagnostic value in HCC.

In addition to fucosylation, sialylation plays an essential role in cell–cell recognition, cell adhesion, antigenicity, protein targeting and invasion [46–48], is closely associated with HCC [49]. In the present study, sialylation levels were continuously elevated in CHB, LC and HCC compared to HC (Fig. 3D), consistent with the increased sialylation levels in serum samples of HCC patients [50]. Moreover, sialylated glycoproteins were documented to be dysregulated in the progression of HCC, including AFP [51] and paraoxonase 1 [52]. In the present study, 39 sialylated glycopeptides were continuously increased in HCC progression (Fig. S3), which were consisted of 26 sialylated N-glycans and 16 peptides from 23 glycoproteins. Among these glycopeptides, SERPINA1-271-HexNAc(4)Hex(5)NeuAc(1) was identified with highest PSM score. Aligning with this change, sialylated SERPINA1 were up-regulated in early-stage oropharyngeal squamous cell carcinoma [53] and in metastatic HCC compared to non-metastatic HCC group [54], suggesting that sialylated SERPINA1 was closely associated with HCC.

Therefore, we speculate that changes in serum IgG and IgA glycosylation may closely correlate to the progression of HCC, and act as complementary techniques to improve diagnosis.

Abbreviation

HCC	Hepatocellular carcinoma
HBV	Hepatitis B virus
GEO	Gene Expression Omnibus
FUTs	Fucosyltransferases
HBV-HCC	HBV-associated HCC
AFP	Alpha-fetoprotein
β1,6-GlcNAc	β1,6-N-acetylglucosamine
TF	Transferrin
A1AT	Alpha-1-anti-trypsin
CHB	Chronic hepatitis B
LC	Liver cirrhosis
HC	Healthy controls
NCBI	National Center for Biotechnology Information
RT-qPCR	Quantitative reverse transcription PCR
DTT	Dithiothreitol
IAM	Iodoacetamide
SPE	Solid phase extraction
DHB	2,5-Dihydroxybenzoic acid
LCA	Lens Culinaries Agglutinin
SD	Standard deviation
DEGGs	Differentially expressed glyco-genes
PLS-DA	Partial Least Squares Discrimination Analysis
PPI	Protein–protein interaction
DEGPeps	Differentially expressed glycopeptides

Supplementary Information

The online version contains supplementary material available at https://doi.org/10.1186/s12964-024-01569-y.

Additional file 1: Fig. S1. PPI network of other DEGGs. The PPI network of DEGGs performed by the STRING database and cytoscape tools. **Fig. S2.** Functional enrichment analysis of glycopeptides from cluster II (A), III (B) and IV (C). **Fig. S3.** Heatmap of sialylated N-glycans on intact glycopeptides from cluster I. PSMs of the intact glycopeptides, comprising of different glycans (bottom) and their glycosite locations in different glycoproteins (right) are exhibited in the heat map.

Additional file 2: Table 1. Characteristics of 100 participants clincal data of glycomics. **Table 2.** Characteristics of 80 of 100 participants clincal data of glycoproteomics. **Table 3.** Primers of glycan-related genes. **Table 4.** Differentially expressed glyco-genes in GSE135631 and GSE94660. **Table 5.** Identified N-glycans in HC, CHB, LC and HCC serum samples. **Table 6.** Identified glycopeptides in HC, CHB, LC and HCC serum samples. **Table 7.** Differentially expressed intact glycopeptides from cluster I-IV. **Table 8.** Differentially expressed proteins in CHB, LC and HBV-HCC compared HC. **Table 9.** Glycosylation site occupancy of glycopeptides in HC, CHB, LC and HBV-HCC.

Acknowledgements
Not applicable

Authors' contributions
Zengqi Tan, Yue Zhou and Feng Guan designed the experiments. Zengqi Tan, Zhuo Li, Na Zhang, Zewen Dong, Yunyun Yang and Jing Li performed experiments and data analysis. Xin Wang, Jian Zhou and Juan Gao collected samples. Zengqi Tan, Zhuo Li and Na Zhang wrote the manuscript.

Funding
This work was supported by the National Natural Science Foundation of China (Grant No. 32271338 and 82102471), Shaanxi Provincial Health Research Fund Project (Grant No. 2022A019), and Shaanxi Fundamental Science Research Project for Chemistry & Biology (Grand No. 22JHQ077).

Availability of data and materials
Raw data has been deposited into a jPOSTrepo repository [55] The accession link was https://repository.jpostdb.org/preview/2022.

Declarations

Ethics approval and consent to participate
This study was approved by The First Affiliated Hospital of Xi'an Medical University Ethics Committee (approval No. XYLS2021046) and all subjects signed informed consent.

Consent for publication
Not applicable.

Competing interests
The authors declare no competing interests.

Received: 27 October 2023 Accepted: 12 March 2024
Published online: 01 April 2024

References

1. Vogel A, Meyer T, Sapisochin G, Salem R, Saborowski A. Hepatocellular carcinoma. Lancet. 2022;400:1345–62.
2. Zhang CH, Cheng Y, Zhang S, Fan J, Gao Q. Changing epidemiology of hepatocellular carcinoma in Asia. Liver Int. 2022;42:2029–41.
3. Li TY, Yang Y, Zhou G, Tu ZK. Immune suppression in chronic hepatitis B infection associated liver disease: a review. World J Gastroenterol. 2019;25:3527–37.
4. Yue T, Zhang Q, Cai T, Xu M, Zhu H, Pourkarim MR, et al. Trends in the disease burden of HBV and HCV infection in China from 1990–2019. Int J Infect Dis. 2022;122:476–85.
5. Wang H, Men P, Xiao Y, Gao P, Lv M, Yuan Q, et al. Hepatitis B infection in the general population of China: a systematic review and meta-analysis. BMC Infect Dis. 2019;19:811.

6. Evans AA, Chen G, Ross EA, Shen FM, Lin WY, London WT. Eight-year follow-up of the 90,000-person Haimen City cohort: I. Hepatocellular carcinoma mortality, risk factors, and gender differences. Cancer Epidemiol Biomarkers Prev. 2002;11:369–76.
7. Kanda T, Goto T, Hirotsu Y, Moriyama M, Omata M. Molecular Mechanisms Driving Progression of Liver Cirrhosis towards Hepatocellular Carcinoma in Chronic Hepatitis B and C Infections: a review. Int J Mol Sci. 2019;20:1358.
8. Seeger C, Mason WS. Molecular biology of hepatitis B virus infection. Virology. 2015;479–480:672–86.
9. Hanif H, Ali MJ, Susheela AT, Khan IW, Luna-Cuadros MA, Khan MM, et al. Update on the applications and limitations of alpha-fetoprotein for hepatocellular carcinoma. World J Gastroenterol. 2022;28:216–29.
10. Luo P, Wu S, Yu Y, Ming X, Li S, Zuo X, et al. Current Status and Perspective Biomarkers in AFP Negative HCC: Towards Screening for and Diagnosing Hepatocellular Carcinoma at an Earlier Stage. Pathol Oncol Res. 2020;26:599–603.
11. Hu KQ, Kyulo NL, Lim N, Elhazin B, Hillebrand DJ, Bock T. Clinical significance of elevated alpha-fetoprotein (AFP) in patients with chronic hepatitis C, but not hepatocellular carcinoma. Am J Gastroenterol. 2004;99:860–5.
12. Silsirivanit A. Glycosylation markers in cancer. Adv Clin Chem. 2019;89:189–213.
13. Kailemia MJ, Park D, Lebrilla CB. Glycans and glycoproteins as specific biomarkers for cancer. Anal Bioanal Chem. 2017;409:395–410.
14. Hirata T, Kizuka Y. N-Glycosylation. Adv Exp Med Biol. 2021;1325:3–24.
15. Huang Y, Zhang HL, Li ZL, Du T, Chen YH, Wang Y, et al. FUT8-mediated aberrant N-glycosylation of B7H3 suppresses the immune response in triple-negative breast cancer. Nat Commun. 2021;12:2672.
16. Miao Z, Cao Q, Liao R, Chen X, Li X, Bai L, et al. Elevated transcription and glycosylation of B3GNT5 promotes breast cancer aggressiveness. J Exp Clin Cancer Res. 2022;41:169.
17. Scott DA, Drake RR. Glycosylation and its implications in breast cancer. Expert Rev Proteomics. 2019;16:665–80.
18. Radovani B, Gudelj I. N-Glycosylation and Inflammation; the Not-So-Sweet Relation. Front Immunol. 2022;13:893365.
19. Tena J, Tang X, Zhou Q, Harvey D, Barajas-Mendoza M, Jin LW, et al. Glycosylation alterations in serum of Alzheimer's disease patients show widespread changes in N-glycosylation of proteins related to immune function, inflammation, and lipoprotein metabolism. Alzheimers Dement (Amst). 2022;14:e12309.
20. Conroy LR, Hawkinson TR, Young LEA, Gentry MS, Sun RC. Emerging roles of N-linked glycosylation in brain physiology and disorders. Trends Endocrinol Metab. 2021;32:980–93.
21. Rudman N, Gornik O, Lauc G. Altered N-glycosylation profiles as potential biomarkers and drug targets in diabetes. FEBS Lett. 2019;593:1598–615.
22. Stambuk T, Gornik O. Protein Glycosylation in Diabetes. Adv Exp Med Biol. 2021;1325:285–305.
23. Rudman N, Kifer D, Kaur S, Simunovic V, Cvetko A, Pociot F, et al. Children at onset of type 1 diabetes show altered N-glycosylation of plasma proteins and IgG. Diabetologia. 2022;65:1315–27.
24. West CA, Wang M, Herrera H, Liang H, Black A, Angel PM, et al. N-Linked glycan branching and fucosylation are increased directly in hcc tissue as determined through in situ glycan imaging. J Proteome Res. 2018;17:3454–62.
25. Kim KJ, Kim YW, Hwang CH, Park HG, Yang YH, Koo M, et al. A MALDI-MS-based quantitative targeted glycomics (MALDI-QTaG) for total N-glycan analysis. Biotechnol Lett. 2015;37:2019–25.
26. Shan M, Yang D, Dou H, Zhang L. Fucosylation in cancer biology and its clinical applications. Prog Mol Biol Transl Sci. 2019;162:93–119.
27 Kizuka Y, Taniguchi N. Enzymes for N-Glycan branching and their genetic and nongenetic regulation in cancer. Biomolecules. 2016;6:25.
28. Zhou X, Zhang J, Song Z, Lu S, Yu Y, Tian J, et al. ExoTracker: a low-pH-activatable fluorescent probe for labeling exosomes and monitoring endocytosis and trafficking. Chem Commun (Camb). 2020;56:14869–72.
29. Ma J, Sanda M, Wei R, Zhang L, Goldman R. Quantitative analysis of core fucosylation of serum proteins in liver diseases by LC-MS-MRM. J Proteomics. 2018;189:67–74.
30. Cao L, Zhou Y, Li X, Lin S, Tan Z, Guan F. Integrating transcriptomics, proteomics, glycomics and glycoproteomics to characterize paclitaxel resistance in breast cancer cells. J Proteomics. 2021;243:104266.
31. Ceroni A, Maass K, Geyer H, Geyer R, Dell A, Haslam SM. GlycoWorkbench: a tool for the computer-assisted annotation of mass spectra of glycans. J Proteome Res. 2008;7:1650–9.
32. Wang R, Liu Y, Wang C, Li H, Liu X, Cheng L, et al. Comparison of the methods for profiling N-glycans-hepatocellular carcinoma serum glycomics study. RSC Adv. 2018;8:26116–23.
33. Ramachandran P, Xu G, Huang HH, Rice R, Zhou B, Lindpaintner K, et al. Serum Glycoprotein Markers in Nonalcoholic Steatohepatitis and Hepatocellular Carcinoma. J Proteome Res. 2022;21:1083–94.
34. Tsai TH, Wang M, Di Poto C, Hu Y, Zhou S, Zhao Y, et al. LC-MS profiling of N-Glycans derived from human serum samples for biomarker discovery in hepatocellular carcinoma. J Proteome Res. 2014;13:4859–68.
35. Zhou J, Yang W, Hu Y, Höti N, Liu Y, Shah P, et al. Site-Specific Fucosylation Analysis Identifying Glycoproteins Associated with Aggressive Prostate Cancer Cell Lines Using Tandem Affinity Enrichments of Intact Glycopeptides Followed by Mass Spectrometry. Anal Chem. 2017;89:7623–30.
36. Dalal K, Dalal B, Bhatia S, Shukla A, Shankarkumar A. Analysis of serum Haptoglobin using glycoproteomics and lectin immunoassay in liver diseases in Hepatitis B virus infection. Clin Chim Acta. 2019;495:309–17.
37. Guo L, Wan L, Hu Y, Huang H, He B, Wen Z. Serum N-glycan profiling as a diagnostic biomarker for the identification of hepatitis B virus-associated hepatocellular carcinoma. J Gastrointest Oncol. 2022;13:344–54.
38. Comunale MA, Lowman M, Long RE, Krakover J, Philip R, Seeholzer S, et al. Proteomic analysis of serum associated fucosylated glycoproteins in the development of primary hepatocellular carcinoma. J Proteome Res. 2006;5:308–15.
39. Block TM, Comunale MA, Lowman M, Steel LF, Romano PR, Fimmel C, et al. Use of targeted glycoproteomics to identify serum glycoproteins that correlate with liver cancer in woodchucks and humans. Proc Natl Acad Sci U S A. 2005;102:779–84.
40. Yao W, Wang K, Jiang Y, Huang Z, Huang Y, Yan H, et al. Serum profile of low molecular weight fucosylated glycoproteins for early diagnosis of hepatocellular carcinoma. Oncol Lett. 2020;20:1597–606.
41. Liu XE, Desmyter L, Gao CF, Laroy W, Dewaele S, Vanhooren V, et al. N-glycomic changes in hepatocellular carcinoma patients with liver cirrhosis induced by hepatitis B virus. Hepatology. 2007;46:1426–35.
42. Fang M, Zhao YP, Zhou FG, Lu LG, Qi P, Wang H, et al. N-glycan based models improve diagnostic efficacies in hepatitis B virus-related hepatocellular carcinoma. Int J Cancer. 2010;127:148–59.
43. Yang S, Cui M, Liu Q, Liao Q. Glycosylation of immunoglobin G in tumors: Function, regulation and clinical implications. Cancer Lett. 2022;549:215902.
44. Yi CH, Weng HL, Zhou FG, Fang M, Ji J, Cheng C, et al. Elevated core-fucosylated IgG is a new marker for hepatitis B virus-related hepatocellular carcinoma. Oncoimmunology. 2015;4:e1011503.
45. Zhang S, Cao X, Liu C, Li W, Zeng W, Li B, et al. N-glycopeptide Signatures of IgA(2) in Serum from Patients with Hepatitis B Virus-related Liver Diseases. Mol Cell Proteomics. 2019;18:2262–72.
46. Schauer R. Achievements and challenges of sialic acid research. Glycoconj J. 2000;17:485–99.
47. Bull C, Stoel MA, den Brok MH, Adema GJ. Sialic acids sweeten a tumor's life. Cancer Res. 2014;74:3199–204.
48. Bull C, den Brok MH, Adema GJ. Sweet escape: sialic acids in tumor immune evasion. Biochim Biophys Acta. 2014;1846:238–46.
49. Zou X, Lu J, Deng Y, Liu Q, Yan X, Cui Y, et al. ST6GAL1 inhibits metastasis of hepatocellular carcinoma via modulating sialylation of MCAM on cell surface. Oncogene. 2023;42:516–29.
50. Goldman R, Ressom HW, Varghese RS, Goldman L, Bascug G, Loffredo CA, et al. Detection of hepatocellular carcinoma using glycomic analysis. Clin Cancer Res. 2009;15:1808–13.
51. Mondal G, Chatterjee U, Chawla YK, Chatterjee BP. Alterations of glycan branching and differential expression of sialic acid on alpha fetoprotein among hepatitis patients. Glycoconj J. 2011;28:1–9.
52. Sun C, Chen P, Chen Q, Sun L, Kang X, Qin X, et al. Serum paraoxonase 1 heteroplasmon, a fucosylated, and sialylated glycoprotein in distinguishing early hepatocellular carcinoma from liver cirrhosis patients. Acta Biochim Biophys Sin (Shanghai). 2012;44:765–73.
53. Dickinson A, Joenvaara S, Tohmola T, Renkonen J, Mattila P, Carpen T, et al. Altered microheterogeneity at several N-glycosylation sites in OPSCC in constant protein expression conditions. FASEB Bioadv. 2024;6:26–39.

54. Qin X, Chen Q, Sun C, Wang C, Peng Q, Xie L, et al. High-throughput screening of tumor metastatic-related differential glycoprotein in hepatocellular carcinoma by iTRAQ combines lectin-related techniques. Med Oncol. 2013;30:420.
55. Okuda S, Watanabe Y, Moriya Y, Kawano S, Yamamoto T, Matsumoto M, et al. jPOSTrepo: an international standard data repository for proteomes. Nucleic Acids Res. 2017;45:D1107–11.

Publisher's Note